Nature of the spin-singlet ground state in $CaCuGe_2O_6$

Roser Valentí,[1] T. Saha-Dasgupta,[2] and Claudius Gros[1]
[1]*Fakultät 7, Theoretische Physik, University of the Saarland, 66041 Saarbrücken, Germany*
[2]*S.N. Bose National Centre for Basic Sciences, JD Block, Sector 3, Salt Lake City, Kolkata 700098, India*
(Received 12 April 2002; published 20 August 2002)

We investigate by means of *ab initio* electronic structure analysis and quantum Monte Carlo calculations the scenario where longer-ranged magnetic interactions dominate over short-ranged interactions in the physical description of compounds. This question is discussed, in particular, for the case of $CaCuGe_2O_6$ which shows a spin-singlet behavior induced by third-nearest-neighbor copper pairs.

DOI: 10.1103/PhysRevB.66.054426 PACS number(s): 75.30.Gw, 75.10.Jm, 78.30.−j

There are a few low-dimensional materials which show, contrary to initial intuitive arguments, longer-ranged dominated exchange couplings. Examples include systems like the most discussed 1/5-depleted Heisenberg system CaV_4O_9 (Ref. 1) or the alternating chain compound $(VO)_2P_2O_7$ (Ref. 2). CaV_4O_9, which was originally viewed as an array of weakly coupled square plaquettes of V^{4+} ions, each in a singlet in the ground state, is found to be a system with strongest coupling between next-nearest-neighbor vanadiums[3] as revealed by a recent electronic structure study.[4] In $(VO)_2P_2O_7$ the strongest exchange path[5] is found to be that between two V^{4+} ions through two phosphate groups PO_4 and not between nearest-neighbor vanadium ions V-O-V as was initially thought.[2] From these examples, we learn that the subtle competition between the various interactions can lead to surprises and a microscopic study is needed. A detailed investigation of these systems often unveils interesting properties. One such a system is $CaCuGe_2O_6$, a system related to the spin-Peierls compound $CuGeO_3$.[6]

Susceptibility measurements[7] on $CaCuGe_2O_6$ show the existence of a spin-singlet ground state with an energy gap of 6 meV. But contrary to $CuGeO_3$ where the spin gap opens at the spin-Peierls phase transition,[6] in $CaCuGe_2O_6$ the spin gap is intrinsic and there is no phase transition between 4.2 K and 300 K. Also, inelastic neutron scattering (INS) measurements were carried out on $CaCuGe_2O_6$ powder and the existence of a finite spin gap was confirmed.[8]

A question which neither INS nor susceptibility measurements could clarify was which Cu pairs form the singlets in this material. This issue is of great importance since it determines the magnetic properties of the system. The structure of this material shows an obvious zigzag one-dimensional (1D) chain of spin=1/2 Cu^{2+} ions along the c axis (see Fig. 1). Nevertheless, the magnetization and susceptibility data of Sasago *et al.*[7] are in disagreement with a spin=1/2 Heisenberg chain model. These authors proposed that the spin-gap behavior of the system should be due to longer-distance-formed Cu pairs and considered possible scenarios depending on which Cu pairs were taken into account. Also the analysis of INS powder data led Zheludev *et al.*[8] to conclude that this compound should be described as a weakly interacting dimer system in spite of the fact that the material shows a pronounced 1D arrangement of magnetic ions. Which Cu ions form the pairs, however, could not be strictly defined from the analysis of the above experiments.

It is the purpose of this paper to investigate in detail the singlet nature of this system and why it shows such a behavior. In order to do that we have performed (i) *ab initio* calculations which give us information on the chemical bonding and the electronic structure and (ii) quantum Monte Carlo computations which are used in order to calculate thermodynamical quantities like the susceptibility and magnetization in this material.

Crystal structure. $CaCuGe_2O_6$ crystallizes in the monoclinic space group $P2_1/c$ with lattice parameters $a=10.198$ Å, $b=9.209$ Å, $c=5.213$ Å, and $\beta=105.73°$, and it contains four formula units per primitive unit cell.[9] The copper ions are all equivalent and form Jahn-Teller-distorted octahedra with the surrounding oxygens and they build zigzag chains along the c direction [see Fig. 1(a)] by sharing an edge of the octahedra. Intercalated between these chains are the Ge and Ca ions. The distances between two nearest-neighbor (NN) Cu within the same chain is 3.072 Å and the Cu-O-Cu angles in these chains are 92° for the Cu-O1A-Cu angle and 98° for the Cu-O1B-Cu angle (see Fig. 3 and Ref. 10 for the oxygen notation). The Cu-Cu distance within the second-NN pair which are also located in the same zigzag chain is 5.213 Å. The third and fourth NN are formed by Cu atoms belonging to neighboring bc planes (see Fig. 1). The distances between two neighboring bc planes alternate between $d=4.462$ Å and $d^*=5.354$ Å, giving

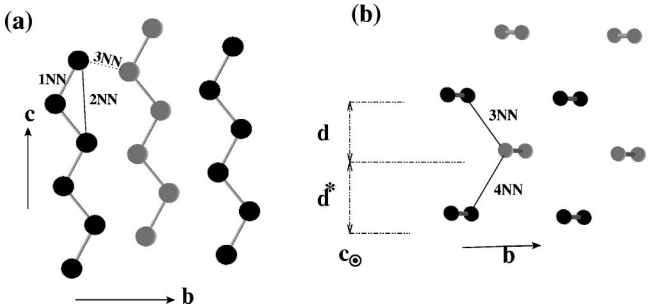

FIG. 1. (a) Projection on the bc plane of the Cu zigzag chains in $CaCuGe_2O_6$, where the 1NN, 2NN, and 3NN Cu pairs are indicated. The chains alternate between two neighboring bc plans (denoted by black and gray balls). (b) Projection on the ab plane of the Cu sites, where the 3NN and 4NN Cu pairs are indicated. The linked Cu sites correspond to 1NN. d and d^* denote the distances between two neighboring bc planes.

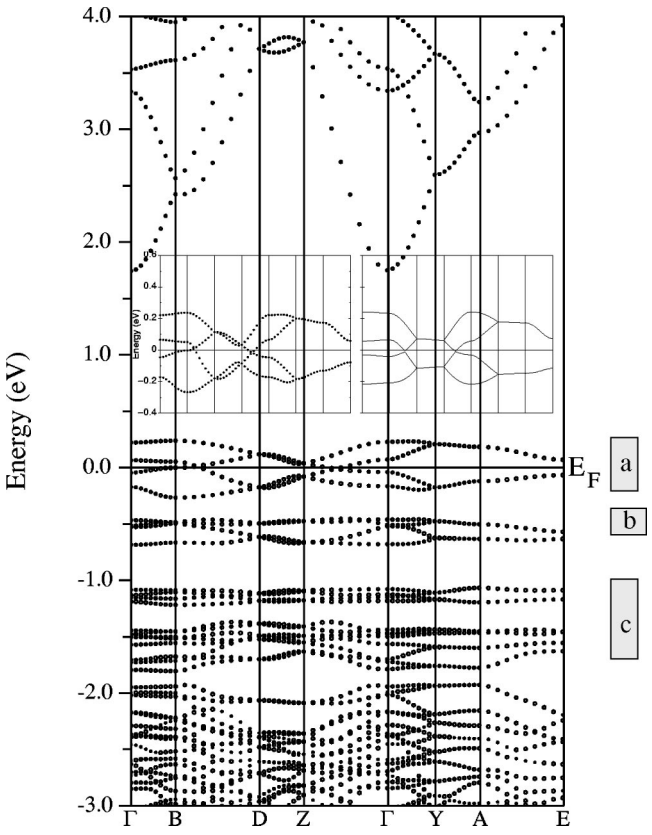

FIG. 2. DFT results for $CaCuGe_2O_6$. The path is along $\Gamma=(0,0,0)$, $B=(-\pi,0,0)$, $D=(-\pi,0,\pi)$, $Z=(0,0,\pi)$, Γ, $Y=(0,\pi,0)$, $A=(-\pi,\pi,0)$, and $E=(-\pi,\pi,\pi)$. Also shown in rectangles is the Cu-band character (in the local coordinate system) $a=d_{x^2-y^2}$, $b=d_{3z^2-1}$, and $c=d_{xy}$, d_{xz}, d_{yz}. Shown in the inset are the four DFT bands close to the Fermi level (left panel) and the corresponding *downfolded* TB bands considering up to 4 NN hopping (right panel) along the same path.

rise to third NN and fourth-NN distances of 5.549 Å and 6.213 Å, respectively.

Band structure. We have performed an *ab initio* study based on the density-functional theory (DFT) in the generalized gradient approximation[11] (GGA) in order to derive the electronic properties of $CaCuGe_2O_6$. Calculations have been performed within the frame-work of both the full-potential linearized augmented-plane-wave (LAPW) method based on the WIEN97 code[12] and the linearized muffin tin orbital (LMTO) method[13] based on the Stuttgart TBLMTO-47 code. The results of the band-structure calculations show four narrow bands close to the Fermi level with a bandwidth of ~ 0.5 eV, having predominant Cu $d_{x^2-y^2}$ character (in the local frame) admixed with oxygen contributions. These bands are half-filled and strong correlation effects should explain the insulating ground state in this compound. These bands are separated by an energy gap of about 0.3 eV from the valence-band set and a gap of about 2 eV from the conduction bands (see Fig. 2).

Effective model. We have performed a LMTO-based downfolding and tight-binding analysis to derive the (single-particle) tranfer integrals of an effective model for this system.

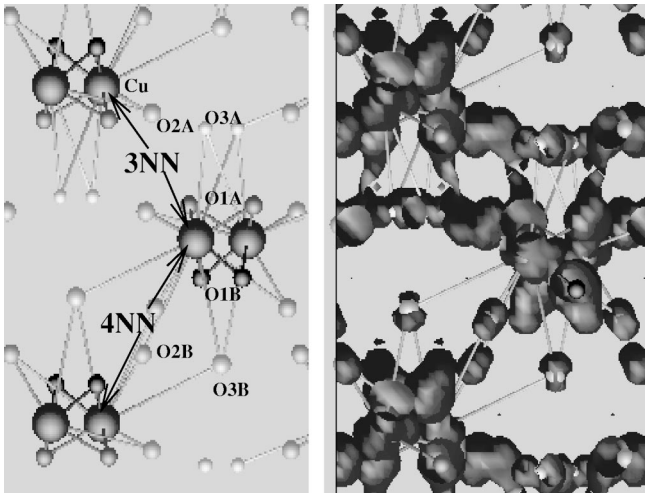

FIG. 3. Electron density plot (right panel) for bands close to the Fermi level in a plane perpendicular to the *c* axis. Note the dominant electron density for the 3NN path with respect to the 4NN path. The left panel shows the crystal structure in the corresponding plane. Big balls represent Cu atoms while small balls represent O atoms. The various nonequivalent oxygens (Refs. 9 and 10) are marked in the figure.

In recent years a new form of the LMTO method has been proposed and implemented[14] which allows to derive few-orbital effective Hamiltonians by keeping only the relevant degrees of freedom and integrating out the irrelevant ones. This procedure amounts to putting the inactive orbitals by downfolding in the tails of the active orbitals kept in the basis. As a result, this takes into account the proper renormalization in the effective interactions between the active orbitals. The effective interactions obtained are therefore unique and given by the intervening interaction paths. Application of the downfolding procedure to $CaCuGe_2O_6$ to derive one orbital (namely, $d_{x^2-y^2}$ per Cu atom) effective model leads to the unambiguous result that the singlet pairs are formed by 3NN Cu pairs. The next important interactions are the 1NN providing a picture of two-dimensional interacting dimers in agreement with susceptibility data and INS. It is to be noted here that a simpleminded tight-binding fitting method with the one-band model is unable to distinguish the relative importance between 3NN and 4NN pairs. Either of the choice of dimer pairs would lead to similar band dispersions though not to the same magnetic behavior. This dominant effect of the 3NN Cu-Cu interaction over the 4NN Cu-Cu interaction originates from the specific orientation of the intervening oxygen atoms between the Cu pairs and their relative hybridization with the Cu $d_{x^2-y^2}$ orbital guided by the magnitude of Cu-O-Cu bond angles and bond lengths. This is supported by the 3D electron density plot shown in Fig. 3 near the Fermi level in a plane perpendicular to the *c* axis. As can be seen, the exchange paths connecting two 3NN coppers are not equivalent to the exchange paths connecting two 4NN coppers. For the considered 3NN Cu-Cu pair the intervening oxygens [predominantly O2A and O3A (Refs. 9 and 10)] provide a well-defined interaction path while for the 4NN Cu-Cu pair the contribution of the inter-

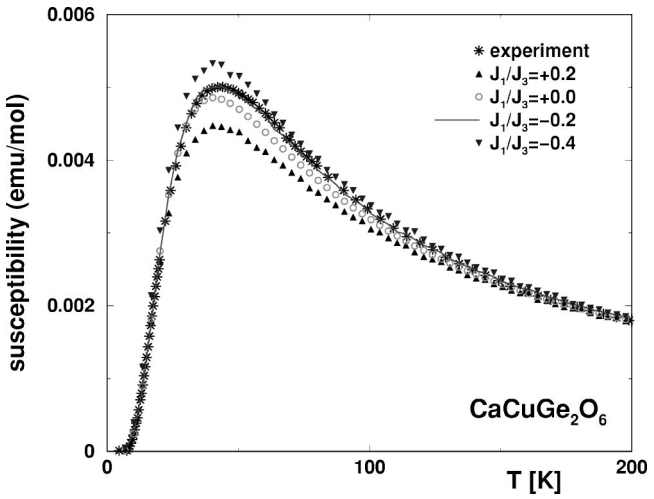

FIG. 4. Temperature dependence of the magnetic susceptibility for $CaCuGe_2O_6$. Shown are the experimental (Ref. 7) data (stars) and the QMC results for the model Eq. (2) for $J_3=67$ K and $J_1/J_3=0.2$ (up triangles, $g=2.076$), $J_1/J_3=0.0$ (open circles, $g=2.032$), $J_1/J_3=-0.2$ (solid line, $g=2.032$), and $J_1/J_3=-0.4$ (down triangles, $g=2.011$).

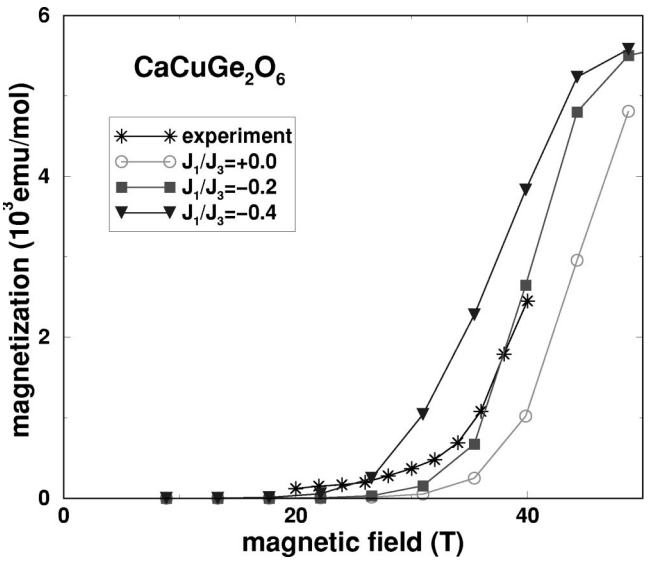

FIG. 5. Magnetization for $CaCuGe_2O_6$ at $T=4.2$ K. Shown are the experimental (Ref. 7) data (stars) and the QMC results for the model Eq. (2) for $J_1/J_3=0.0$ (open circles), $J_1/J_3=-0.2$ (solid squares), and $J_1/J_3=-0.4$ (down triangles) with the same parameters as in Fig. (4).

vening oxygens (predominantly O2B and O3B) is much smaller, leading to almost disconnected Cu^{2+} ions. This fact is also supported by the partial density of states (DOS) analysis at the Fermi level of the oxygen contribution where we observe that the contribution coming from O2B and O3B orbitals is almost negligible compared to that of O2A and O3A.

The *downfolded* TB bands are represented by a Hamiltonian of the form

$$H_{TB}=\sum_{(i,j)} t_{ij}(c_i^{\dagger}c_j+\text{H.c.}), \tag{1}$$

where the t_{ij} are hopping matrix elements between Cu neighbors i and j. We have considered hopping matrix elements up to fourth-nearest-neighbor (see Fig. 1) t_1, t_2, t_3, and t_4 (the subindex denotes 1NN, 2NN, 3NN, and 4NN, respectively). The values derived for this effective model were found to be $t_1=0.068$ eV, $t_2=0.008$ eV, $t_3=0.088$ eV, and $t_4=0.004$ eV. In the inset of Fig. 2 we show the comparison of the DFT bands to the *downfolded* TB bands considering t_1, t_2, t_3, and t_4 hoppings only. The band splitting along the path DZ is reproduced by considering longer-ranged hopping matrix elements.

An estimate of the exchange integral related to the most dominating 3NN interaction parameter t_3 can be obtained by using the relation $J_3\sim 4t_3^2/U$ where U is the effective on-site Coulomb repulsion. A value of $U\sim 4.2$ eV was proposed for $CuGeO_3$ by mapping experimental data onto a one-band description.[15] Assuming that this value is similar for $CaCuGe_2O_6$, we get a value of $J_3\sim 86$ K.

Susceptibility and magnetization. The description for $CaCuGe_2O_6$ obtained from the previous first-principles calculation is that of a system of interacting dimers. In order to check this result we have analyzed both the susceptibility as well as the magnetization behavior of this material by considering the following model:

$$H_{eff}=J_3\sum_{\langle i,j\rangle} S_iS_j+J_1\sum_{(i,j)} S_iS_j, \tag{2}$$

where J_3 and J_1 are the exchange integrals between 3NN and 1NN as illustrated in Fig. 1. The analysis of the model has been done by quantum Monte Carlo (QMC) simulations (stochastic series expansion[16,17]) on 20×40 lattices. We found an optimal value for $J_3=67$ K, very close to the value 68 K proposed by Sasago *et al.*[7] We find clear evidence for a weak ferromagnetic interdimer coupling $J_1<0$, as shown in Fig. 4. The optimal value is $J_1=-0.2J_3$. The g factor was determined by fitting the QMC results for the susceptibility $\chi^{(th)}=\langle(S^z-\langle S^z\rangle)^2\rangle$ with the experimental susceptibility χ (in [emu/mol]) at high temperatures via[18] $\chi\equiv 0.375(g^2/J)\chi^{(th)}$. The optimal g factor was found to be $g=2.032$, close to the value 2.07 proposed earlier.[7]

Sasago *et al.* measured the magnetization curve for $CaCuGe_2O_6$ as a function of an applied magnetic field at $T=4.2$ K. With the stochastic series expansion QMC method it is possible to simulate quantum-spin models in an external field,[17] although these simulations become very hard near saturation. We present the results of this simulation in Fig. 5, for the same parameters we used for evaluating the susceptibility, together with the experimental results. It is very reassuring that $J_1=-0.2J_3$ is again the optimal parameter set.

The phase diagram of model Eq. (2) is very interesting by itself. In the limit $J_3=0$ it consists of decoupled J_1-chains [see Fig. 1(a)] either antiferromagnetic or ferromagnetic for $J_1>0$ or $J_1<0$, respectively. In both cases the excitation spectrum is gapless, while it shows a gap in the limit J_1

$=0$, $J_3 \neq 0$ (dimer phase). We therefore expect two quantum critical points connecting these two regions. We have investigated the phase diagram and found the critical coupling strength to be $J_1 \simeq 0.55 J_3$ and $J_1 \simeq -0.9 J_3$, respectively. The parameter range for $CaCuGe_2O_6$ is away from these two critical points.

Discussion and conclusions. The analysis of the electronic structure of $CaCuGe_2O_6$ by first-principles calculations as well as the examination of susceptibility and magnetization data by the QMC method leads to a unique description of this material as a system of dimers formed by 3NN magnetic spin$=1/2$ Cu^{2+} ions with ferromagnetic (1NN) interdimer couplings. The ferromagnetic nature of the 1NN coupling is more subtle to understand than in other edge-sharing Cu-O systems[19] since due to the strong distortion of the Cu octahedron, this coupling proceeds through two pathes with angles 92° and 98°. These two paths can provide in principle competing ferromagnetic[20] and antiferromagnetic couplings, respectively. The analysis of the susceptibility and magnetization behavior shows nonetheless a clear effective ferromagnetic coupling. In this system, since the primary role is played by the 3NN Cu pairs, the role of the possible frustrating 2NN term to the 1NN interaction is secondary, unlike the case of the related spin-Peierls material $CuGeO_3$. The strength of the magnetic exchange integrals has been obtained from the analysis of the susceptibility and the magnetization data with very good agreement between these two measurements. DFT calculations overestimate the value of J_1, which is not surprising;[21] nonetheless, the physical picture of this material is correctly provided by DFT *+downfolding* TB analysis.

In conclusion, by analyzing the electronic and magnetic properties of $CaCuGe_2O_6$ we have been able to provide a physical picture of the system as well as a microscopic description of the singlet nature in this material. The combination of *ab initio* techniques with many-body methods (QMC) can unambigously determine the microscopic behavior of a system as has been shown for $CaCuGe_2O_6$ in particular.

$CaCuGe_2O_6$ shows an interesting spin-gap behavior and we believe that experiments under the application of a magnetic field would be desirable to investigate the possible appearance of long-range order in the system. Moreover, the 2D interaction model provided by this system, Eq. (2), is interesting *per se* since it shows two quantum critical points as a function of the strength quotient J_1/J_3.

One of us (R.V.) thanks the German Research Foundation (DFG) for financial support.

[1] S. Taniguchi, T. Nishikawa, Y. Yasui, Y. Kobayashi, M. Sato, T. Nishioka, M. Kontani, and K. Sano, J. Phys. Soc. Jpn. **64**, 2758 (1995).

[2] D.C. Johnston, J.W. Johnson, D.P. Goshorn, and A.J. Jacobson, Phys. Rev. B **35**, 219 (1987).

[3] The nearest-neighbor coupling in CaV_4O_9 is argued to be small due to strong cancellation among the various superexchange processes.

[4] W.E. Pickett, Phys. Rev. Lett. **79**, 1746 (1997); C.S. Hellberg, W.E. Pickett, L.L. Boyer, H.T. Stokes, and M.J. Mehl, J. Phys. Soc. Jpn. **68**, 3489 (1999).

[5] D.A. Tennant, S.E. Nagler, A.W. Garrett, T. Barnes, and C.C. Torardi, Phys. Rev. Lett. **78**, 4998 (1997).

[6] M. Hase, I. Terasaki, and K. Uchinokura, Phys. Rev. Lett. **70**, 3651 (1993).

[7] Y. Sasago, M. Hase, K. Uchinokura, M. Tokunaga, and N. Miura, Phys. Rev. B **52**, 3533 (1995).

[8] A. Zheludev, G. Shirane, Y. Sasago, M. Hase, and K. Uchinokura, Phys. Rev. B **53**, 11 642 (1996).

[9] M. Behruzi, K.-H. Breuer, and W. Eysel, Z. Kristallogr. **176**, 205 (1986).

[10] There are six nonequivalent oxygens in the $CaCuGe_2O_6$ structure, O1A, O2A, O3A, O1B, O2B, O3B following the notation of Behruzi *et al.* (Ref. 9).

[11] J.P. Perdew, K. Burke, and M. Ernzerhof, Phys. Rev. Lett. **77**, 3865 (1996).

[12] P. Blaha, K. Schwarz, and J. Luitz, computer code WIEN97, A Full Potential Linearized Augmented Plane Wave Package for Calculating Crystal Properties, Karlheinz Schwarz, Technical University of Wien, Vienna, 1999 [updated version of P. Blaha, K. Schwarz, P. Sorantin, and S.B. Trickey, Comput. Phys. Commun. **59**, 399 (1990)].

[13] O.K. Andersen, Phys. Rev. B **12**, 3060 (1975).

[14] O.K. Andersen and T. Saha-Dasgupta, Phys. Rev. B **62**, R16 219 (2000) and references therein.

[15] F. Parmigiani, L. Sangaletti, A. Goldoni, U. del Pennino, C. Kim, Z.-X. Shen, A. Revcolevschi, and G. Dhalenne, Phys. Rev. B **55**, 1459 (1997).

[16] A.W. Sandvik, Phys. Rev. B **59**, R14 157 (1999).

[17] A. Dorneich and M. Troyer, Phys. Rev. E **64**, 066701 (2001).

[18] D.C. Johnston, R.K. Kremer, M. Troyer, X. Wang, A. Klümper, S.L. Bud'ko, A.F. Panchula, and P.C. Canfield, Phys. Rev. B **61**, 9558 (2000).

[19] Y. Mizuno *et al.*, Phys. Rev. B **57**, 5326 (1998).

[20] J.B. Goodenough, Phys. Rev. **100**, 564 (1955); J. Kanamori, J. Phys. Chem. Solids **10**, 87 (1959); P.W. Anderson, Solid State Phys. **14**, 99 (1963).

[21] R. Valentí, T. Saha-Dasgupta, J.V. Alvarez, K. Pozgajcic, and C. Gros, Phys. Rev. Lett. **86**, 5381 (2001).